Baghdad Science Journal

Volume 23 | Issue 6 Article 1

6-17-2026

Selective Extraction Based on Molecular Imprinting Polymer for Determination Lorazepam in Pharmaceutical and Biological Samples

Eman W. Ammen
Department of Chemistry, College of Science, University of Baghdad, Baghdad, Iraq AND Scientific Research Commission, Baghdad, Iraq, em_alrawi@yahoo.com

Yehya K. Al-Bayati
Department of Chemistry, College of Science, University of Baghdad, Baghdad, Iraq, yehya.kamal@sc.uobaghdad.edu.iq

How to Cite this Article

Ammen, Eman W. and Al-Bayati, Yehya K. (2026) "Selective Extraction Based on Molecular Imprinting Polymer for Determination Lorazepam in Pharmaceutical and Biological Samples," *Baghdad Science Journal*: Vol. 23: Iss. 6, Article 1.
DOI: https://doi.org/10.21123/2411-7986.5316

BAGHDAD SCIENCE JOURNAL 2026;23(6):1985–2002

RESEARCH ARTICLE

Selective Extraction Based on Molecular Imprinting Polymer for Determination Lorazepam in Pharmaceutical and Biological Samples

Eman W. Ammen [1,2,*], **Yehya K. Al-Bayati** [1]

[1] Department of Chemistry, College of Science, University of Baghdad, Baghdad, Iraq
[2] Scientific Research Commission, Baghdad, Iraq

ABSTRACT

A new and selective method was evaluated for the separation and quantification of lorazepam in pharmaceutical and biological samples utilizing a molecularly imprinted polymer (MIP) as a solid-phase extraction adsorbent material. The molecularly imprinted polymer (MIP) was synthesized via free-radical polymerization with lorazepam as a template and acrylamide as a functional monomer. The synthesized polymers were characterized using UV-visible spectroscopy, Fourier transform infrared spectroscopy, scanning electron microscopy, and thermogravimetric analysis. The adsorption isotherm and Kinetic studies were applied to characterize the adsorption of lorazepam by the synthesized polymers; additionally, the selectivity and reusability of the molecularly imprinted polymer were evaluated. Several parameters affecting solid-phase extraction performance, including adsorbent mass, flow rate, sample pH, sample volume, and the type and volume of the elution solvent were optimized. The proposed approach offers a linear dynamic range of 0.025-0.8 mmol/L, with a correlation coefficient of 0.9990 for lorazepam. The detection and quantification limits were determined to be 0.63 and 2.09 μmol/L, respectively. The suggested approach was well validated for the extraction and quantification of lorazepam in pharmaceutical and biological samples, with recoveries between 95% and 101% and a relative standard deviation of less than 2.5%.

Keywords: Adsorption isotherm, Lorazepam, Molecular imprinting polymer, Solid-phase extraction, UV-visible spectroscopy

Introduction

Lorazepam (LRZ), chemically known as 7-chloro-5-(2-chlorophenyl)-1,3-dihydro-3-hydroxy-2H-1,4-benzodiazepin-2-one, Fig. 1, is classified within the benzodiazepine family of pharmaceuticals.[1] Benzodiazepines (BZDs) are extensively prescribed for their anticonvulsant, anxiolytic, sedative, and muscle relaxant properties, but their use is often associated with dependence, cognitive impairment, and other adverse effects. In recent years, misuse of BZDs has intensified globally, contributing to the broader crisis of prescription drug abuse. Their potent pharmacological action and physicochemical characteristics, such as solubility, tastelessness, and odorlessness, make them prone to abuse and exploitation in criminal activities. Overdoses can cause severe toxicological consequences, highlighting the need for reliable analytical and monitoring approaches.[2]

A variety of analytical techniques have been employed for the determination of benzodiazepines, including lorazepam. These methods include liquid chromatography with tandem mass spectrometry,[2–5] high-performance thin-layer chromatography-mass spectrometry,[6] gas chromatography-mass spectrometry,[7] gas chromatography-tandem mass,[8] and UV-visible spectroscopy.[9,10] Although there have been

Received 10 June 2025; revised 20 September 2025; accepted 11 October 2025.
Available online 17 June 2026

* Corresponding Author.
E-mail addresses: em_alrawi@yahoo.com (E. W. Ammen), yehya.kamal@sc.uobaghdad.edu.iq (Y. K. Al-Bayati).

https://doi.org/10.21123/2411-7986.5316

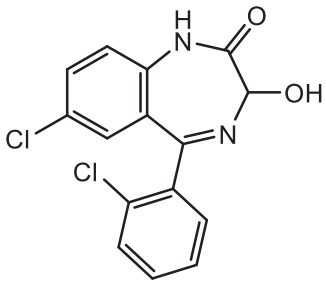

Fig. 1. Lorazepam structure.

substantial improvements in analytical instrumentation, sample preparation procedures are crucial pretreatment steps for complex samples, as they remove a significant number of undesirable substances, thereby enhancing the specificity and selectivity of the method.[11] Supercritical fluid extraction, liquid-phase microextraction, and solid-phase extraction (SPE) are examples of sample pretreatment procedures among these technologies. Solid-phase extraction (SPE) is commonly utilized as a sample pretreatment method. This is due to its low cost, high enrichment efficiency, and simplicity of operation, as well as its low consumption of organic solvents. Conventional SPE has drawbacks, including low filler selectivity. Therefore, it is critical to find new fillers.[12]

Molecular imprinting technology (MIT) is frequently depicted as a method for producing an "artificial lock" that identifies a "molecular key" by simulating enzyme–substrate or antigen–antibody interactions.[13–15] The preparation process of MIPs is typically divided into three parts. The first part involves the preassembly or copolymerization of the template molecule with the functional monomer through specific methods such as non-covalent, covalent, or semi-covalent bonds to form the host–guest complex. The second part involves the addition of a crosslinker and the initiation through specific initiation methods, such as initiator, thermal initiation, photoinitiation, etc., to produce a highly cross-linked polymer. The third part involves the removal of the template molecules through an appropriate method to obtain MIPs with predetermined conformations and specific recognition for the template molecules. MIPs have been extensively employed in the fields of sample pretreatment for the analysis of drugs and various analytes, such as chromatographic separations,[16,17] and sensors[18,19] due to their low cost, simplicity of preparation, chemical stability, and high selectivity.[20,21]

The aim of this research was to synthesize a new lorazepam-MIP, which was utilized as an adsorbent material in solid-phase extraction coupled with UV-Visible spectroscopy. All factors influencing the performance of solid-phase extraction were investigated. The proposed method was successfully applied to the extraction and determination of lorazepam in pharmaceutical and biological samples.

Materials and methods

Reagents and chemicals

Lorazepam and Diazepam were obtained from Sammara (Iraq); Hydrochlorothiazide was supplied by Furat Pharma (Iraq); Acrylamide, Acetic acid, and Sodium hydroxide were sourced from BDH (USA); ethylene glycol dimethacrylate, benzoyl peroxide, and acetone were acquired from Sigma-Aldrich (USA); Ethanol was purchased from Honeywell (USA); Methanol was obtained from PanReac (Spain); and 2-Propanol and hydrochloric acid were sourced from Fulka (Germany).

Instruments

A single-beam UV-visible spectroscopy (UV-1240, Shimadzu, Japan), Fourier transform infrared spectrometer (IR-Affinity-1, Shimadzu, Japan), scanning electron microscope (TM3000 Hitachi Analytical Tabletop, Tokyo, Japan), and thermogravimetric analyzer (SDT Q600, New Castle, DE, USA) were used for the characterization of the prepared polymers.

Synthesis of MIP and NIP

The free-radical polymerization method was used for the synthesis of the molecularly imprinted polymer (MIP) and non-imprinted polymer (NIP). In this polymerization method, 0.2 mmol of LRZ (65.2 mg) was dissolved in 5 mL of a solvent mixture of ethanol and chloroform at a ratio of 2:1 to serve as the template. Following this, 2.35 mmol of acrylamide (167.2 mg) was added to the mixture as the functional monomer; subsequently, 17.53 mmol of ethylene glycol dimethacrylate (3474 mg), used as a cross-linker, and 0.3 mmol of benzoyl peroxide (75 mg), used as the initiator, were dissolved separately in 5 mL of the solvent mixture and incorporated into a screw-cap tube. The mixture was deoxygenated by nitrogen purging for 20 minutes and sealed thoroughly. Polymerization was conducted in a water bath at 60°C for 36 hours. The NIP was synthesized utilizing the identical procedure in the absence of LRZ. To create selective binding sites within the polymer matrix, the resulting MIP was dried, ground using a mortar, and subjected to Soxhlet extraction with a solvent mixture of ethanol and acetic acid at a ratio of 9:1. The extraction process was carried out until LRZ was no longer detected at 319 nm.

Adsorption isotherm and kinetic studies

Column adsorption experiments were conducted to evaluate the adsorption capacity of the synthesized polymers for LRZ.[22] The experiment involved packing 150 mg of MIP/NIP into empty 3 mL solid-phase extraction cartridges. Standard solutions, ranging from 0.05 to 0.9 mmol/L with 3 mL, were then passed through the MIP and NIP cartridges using a peristaltic pump system set to a flow rate of 4 rpm. The concentration of unbound LRZ was determined using a spectrophotometer at 319 nm. The adsorption capacity (Q) for both MIP and NIP for the template LRZ was calculated according to Eq. (1) below:

$$Q_e = \frac{Ci - Ce}{m} V \quad (1)$$

Where Q_e (mg/g) is the mass of LRZ adsorbed onto a unit quantity of dried polymer, C_i (mg/L) is the initial concentration of the LRZ solution, C_e (mg/L) is the equilibrium concentration of the analyte after adsorption, V (L) is the volume of the LRZ solution, and m (g) is the weight of the dry MIP.[23]

Adsorption kinetics were evaluated to assess the rate of the adsorption process of LRZ onto MIP/NIP, which is crucial when constructing an effective adsorption system. The adsorption Kinetics experiments were carried out under the same conditions as the adsorption isotherm experiments but at different contact times (0, 5, 10, 15, 20, 25, and 30 min), with an initial concentration of 0.4 mmol/L of LRZ. The obtained data were analyzed using pseudo-first and second-order models to clarify adsorption processes.

Selectivity of polymers

Polymer selectivity was assessed in the presence of LRZ and two competing drugs (diazepam and hydrochlorothiazide). Binary standard solutions of LRZ and diazepam or hydrochlorothiazide were prepared at a concentration level of 0.2 mmol/L by dissolving the appropriate amounts of the drugs in 100 mL of ethanol. The selectivity experiments were conducted under the same conditions as the adsorption isotherm experiments. The concentration of unbound drugs was determined using a spectrophotometer at a wavelength of 319, 231, and 271 nm for LRZ, diazepam, and hydrochlorothiazide, respectively. The selectivity factor α was calculated using Eq. (2) below:

$$\alpha = \frac{Q_{LRZ}}{Q_{analogue}} \quad (2)$$

Where Q_{LRZ} and $Q_{analogue}$ (mg/g) are the adsorption capacities of the adsorbent for LRZ (template) and the analogue drug, respectively, the imprinting factor (IF) for the synthetic polymers toward each drug was calculated from Eq. (3).

$$IF = \frac{Q_{MIP}}{Q_{NIP}} \quad (3)$$

Where Q_{MIP} and Q_{NIP} (mg/g) represent the capacity of the MIP and NIP toward the target analyte, respectively.[24]

Optimization of MIP-SPE parameters

The molecular imprinting polymer-based solid-phase extraction (MIP-SPE) was utilized as the sample pretreatment method. To enhance the efficiency of analyte extraction, several parameters were optimized, including the amount of MIP, flow rate, sample pH, sample volume, and the type and volume of the elution solvent. The initial sample pretreatment conditions included 100 mg of adsorbent material, a sample volume of 0.5 mL of a 0.4 mmol/L LRZ standard solution at pH 6.0, and 1 mL of ethanol as the elution solvent. Adsorption and desorption processes were conducted using a peristaltic pump set to a flow rate of 4 rpm. Following each extraction, the eluted analyte was analyzed using UV-Vis spectroscopy at a wavelength of 319 nm.

General procedure for LRZ determination

The method involved packing 50 mg of the adsorbent material (MIP) into a 3 mL empty SPE cartridge, which was then conditioned with ethanol. Following this, 0.250 mL of LRZ was introduced into the cartridge. The analyte was eluted using a peristaltic pump set to a flow rate of 2 rpm, followed by the addition of 1.25 mL of ethanol as the analyte elution solvent. The resulting desorbing solution was measured using UV-Vis spectroscopy at a wavelength of 319 nm.

Application to real samples

For the determination of LRZ in pharmaceutical samples, an average mass of 10 tablets (2.00 mg each, SDI-Iraq) from the same batch was recorded. The tablets were finely ground and homogenized in a mortar. A portion of the powdered sample was accurately weighed and dissolved in 25 mL of ethanol. The mixture was then heated and agitated for 10 minutes before being allowed to cool. After cooling, the solution was filtered into a 50 mL volumetric flask, and the volume was adjusted to 50 mL with ethanol to prepare a 10^{-2} mol/L LRZ

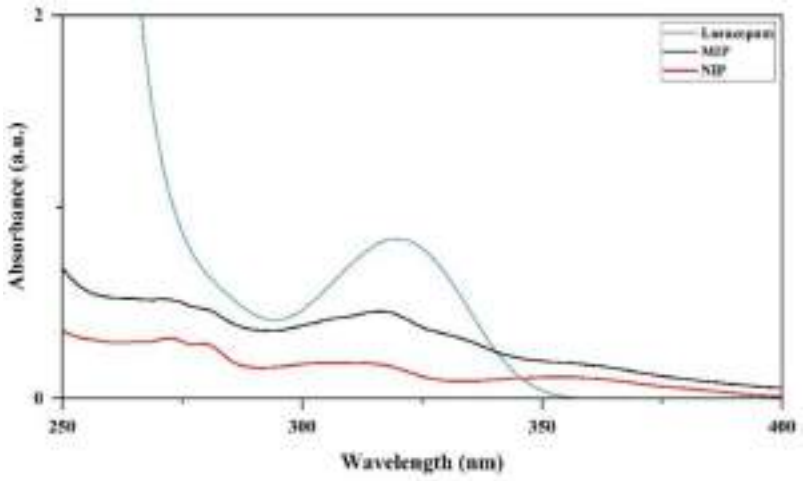

Fig. 2. UV-visible spectra of LRZ, MIP, and NIP.

solution. To achieve the desired LRZ concentrations, further dilutions were performed using ethanol. For the biological samples, drug-free serum samples were obtained from healthy volunteers and stored at –20 ˚C until analysis. The proteins were precipitated by centrifuging the samples at 6000 rpm for 15 minutes after adding acetonitrile at a volume three times that of the serum sample. The supernatant was collected, spiked with the desired concentration of the analyte, and subsequently diluted tenfold.[25] The determination of LRZ in the pharmaceutical and biological samples was conducted according to the general procedure for LRZ determination.

Results and discussion

Characterization of polymers

UV-visible spectroscopy was employed to detect the presence of the template in both MIP and NIP within the wavelength range of 280-400 nm. The objective of this spectral analysis was to differentiate the presence of the drug in the MIP compared to the NIP,[26] as illustrated in Fig. 2. An absorption peak at 319 nm was observed, indicating the presence of LRZ in the MIP. In contrast, this peak was absent in the NIP, confirming the presence of LRZ in the MIP.

FT-IR spectroscopy was employed to characterize the functional groups in the template (LRZ), MIP, and NIP within the 400-4000 cm^{-1} range. The FTIR patterns for the template (LRZ), MIP, and NIP are presented in Fig. 3A strong and broad peak was observed in the range of 3622–3361 cm^{-1} in both the LRZ and MIP spectra. This peak is attributed to the O-H and N-H stretching vibrations, indicating the presence of hydroxyl and amide functional groups in the MIP related to the template. Furthermore, the peaks at 3051 and 3049 cm^{-1} in the LRZ and MIP patterns, respectively, are attributed to the aromatic ring in the drug structure. The peak seen in the range of 2985–2848 cm^{-1} is attributable to the vibration of the C–H stretching mode from LRZ and EGDMA in the template (LRZ), MIP, and NIP. The peaks at 1616 and 1597 cm^{-1} in LRZ and MIP, respectively, are related to the aromatic C=C in the drug structure. The intense peak at 1728 cm^{-1} in MIP and 1726 cm^{-1} in NIP corresponds to the carbonyl ester present in EGDMA. The peaks at 1635 cm^{-1} in MIP and 1670 cm^{-1} in the NIP are related to the aliphatic C=C that are present in the functional monomer and crosslinker. These results indicate that the polymerization process was satisfactory.

Scanning electron microscopy (SEM) was employed to analyze the morphologies of the MIP and NIP particles. The micrographs of the polymers, captured at a magnification of 30000X, are presented in Fig. 4. Both MIP and NIP exhibited irregular surface morphologies, which are a feature of bulk polymerization processes, and the particle size cannot be adequately determined using the ImageJ program.[27] The MIP shows an average pore size of 231.06 nm, which is less than the average pore size of the NIP, 307.53 nm, as illustrated in Figs. 4b and 4d for the MIP and NIP images, respectively. This is attributed to the existence of the template in the MIP. Thermal gravimetric analysis (TGA) was employed to assess the thermal stability of the synthesized polymers by measuring their mass as a function of temperature, as illustrated in Fig. 5. An initial mass loss occurred across all polymers at temperatures below 100°C, which is attributed to moisture and unreacted chemicals that were present during the production of the materials. Following this event, a significant weight

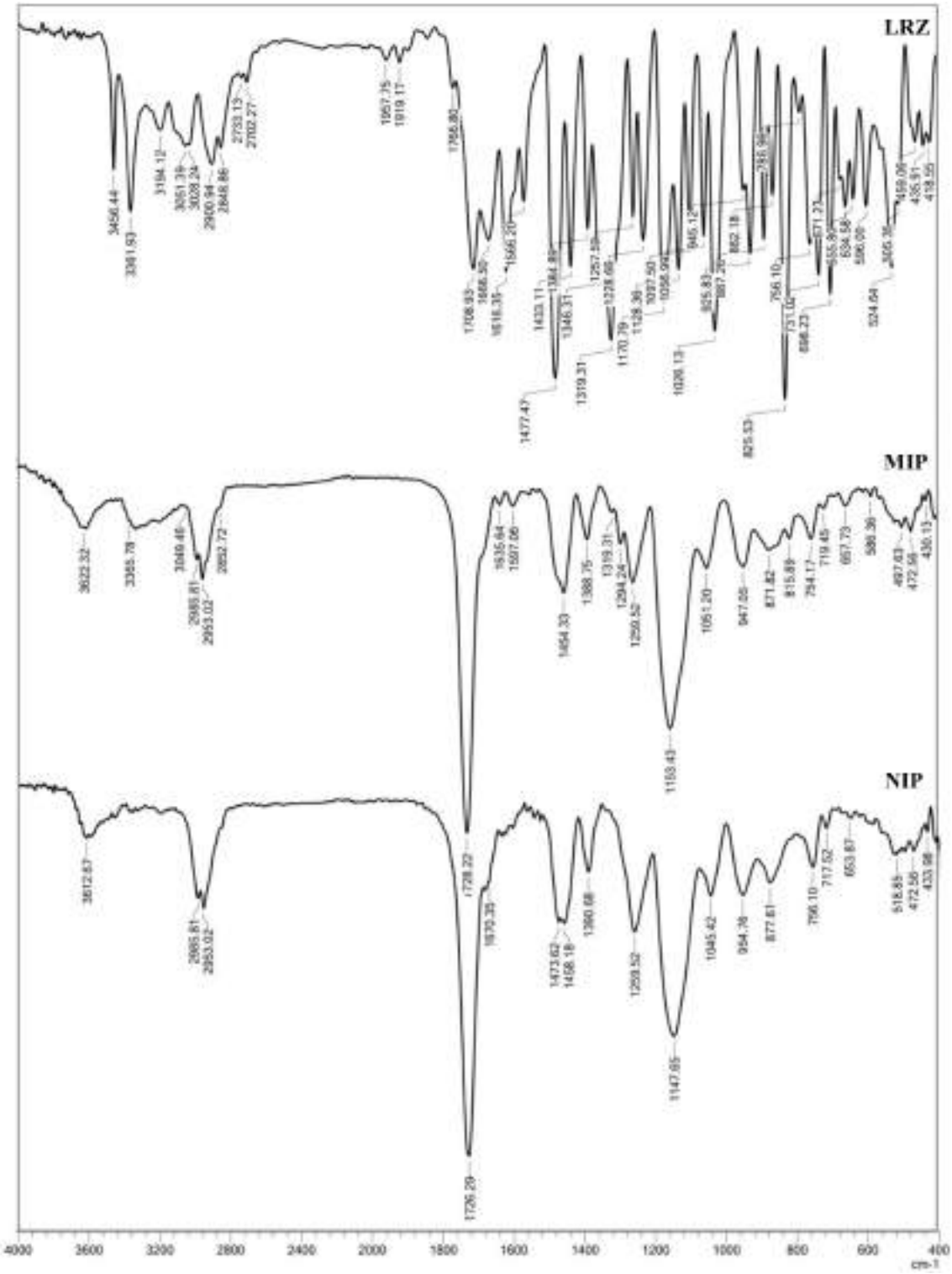

Fig. 3. FT-IR pattern for LRZ, MIP, and NIP.

loss was observed around 420˚C, likely resulting from the decomposition of the materials. Furthermore, it was found that around 10% of the mass was preserved for the MIP after decomposition, whereas approximately 12% was retained for the NIP. The partial elimination of entrapped template molecules during thermal decomposition may be responsible for the lower residue observed in the MIP, which in turn

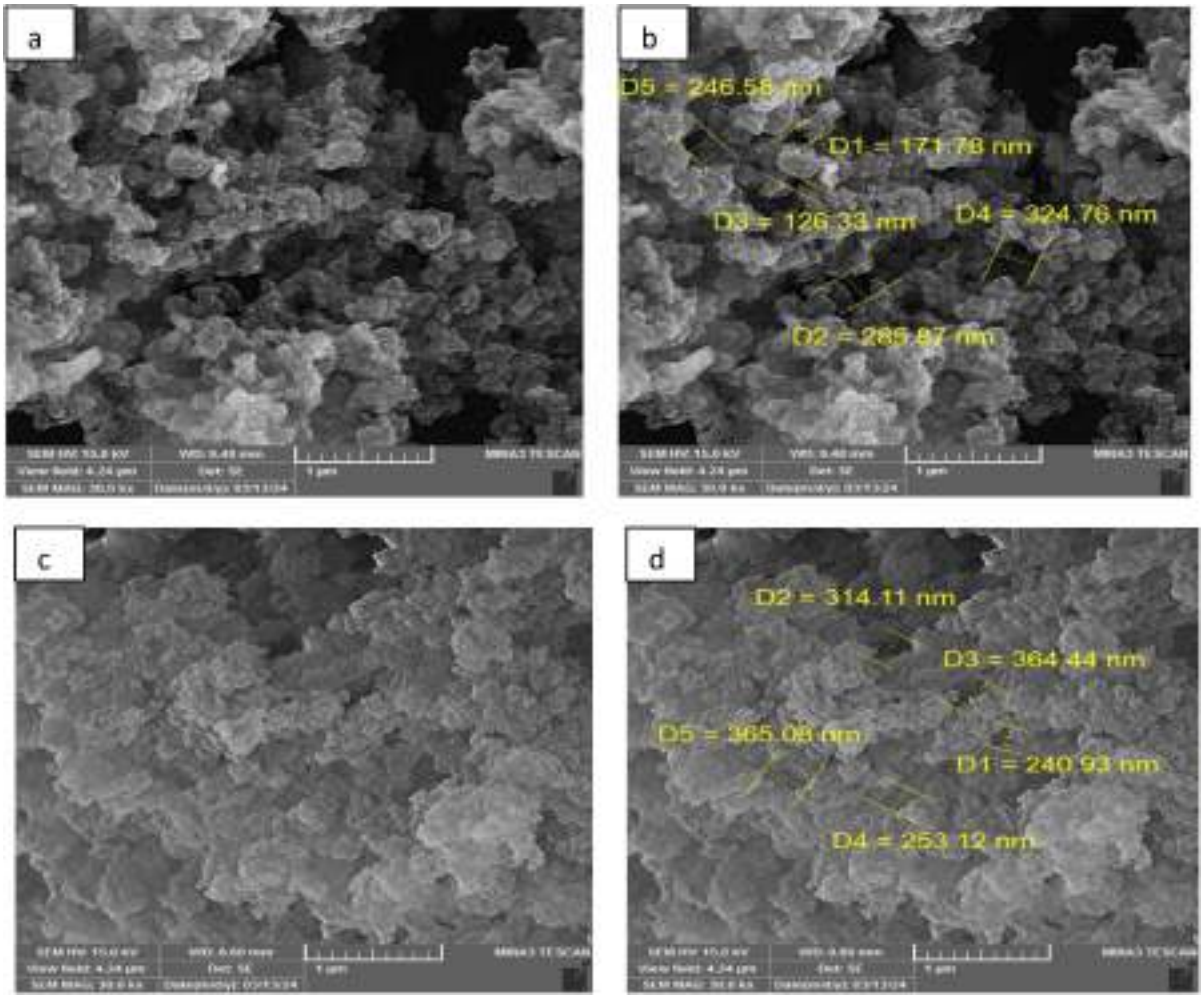

Fig. 4. SEM micrographs of the synthesized polymers at 30,000 × magnification: (a, b) MIP and (c, d) NIP. Images (b) and (d) highlight the pore size diameters of MIP and NIP, respectively.

accelerates the degradation of the imprinted polymer matrix. In contrast, the slightly higher residual mass of the NIP can be attributed to its more compact structure, which is devoid of template-induced porosity, resulting in increased charcoal formation during heating. This discrepancy confirms the impact of template incorporation on the thermal stability of the polymer.[28]

Adsorption isotherm and kinetic studies

Adsorption isotherms were implemented to assess the affinity of the synthesized polymer for LRZ molecules. To achieve this aim, saturation binding experiments were conducted in the concentration range of 0.025-0.9 mmol/L, and the quantity of LRZ molecules adsorbed was determined using Eq. (1). MIP demonstrated a marginally superior adsorption capacity for LRZ in comparison to NIP and the polymer saturation was observed at a concentration of 0.7 mmol/L, confirmed by the linear aspect of the adsorption curve, as illustrated in Fig. 6.

The adsorption process of an analyte on an adsorbent surface is frequently described using the Freundlich and Langmuir models.[25] The Freundlich model applies to heterogeneous adsorption processes or multilayer-type adsorption processes on the adsorbent surface, while the Langmuir model describes a monolayer-type adsorption process on the adsorbent surface.[29] The linear Freundlich equation is expressed as follows:

$$\text{Log } Q_e = \frac{1}{n} \text{ Log } C_e + \text{Log } K_f \quad (4)$$

Where Q_e (mg/g) is the adsorption capacity at equilibrium, and C_e (mg/L) is the equilibrium concentration of LRZ. n and K_f are the parameters related to the intensity and adsorption capacity of the

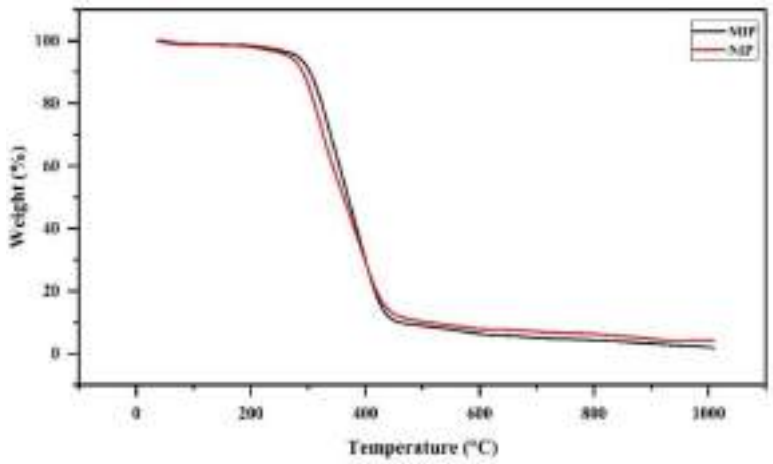

Fig. 5. TGA pattern for MIP and NIP.

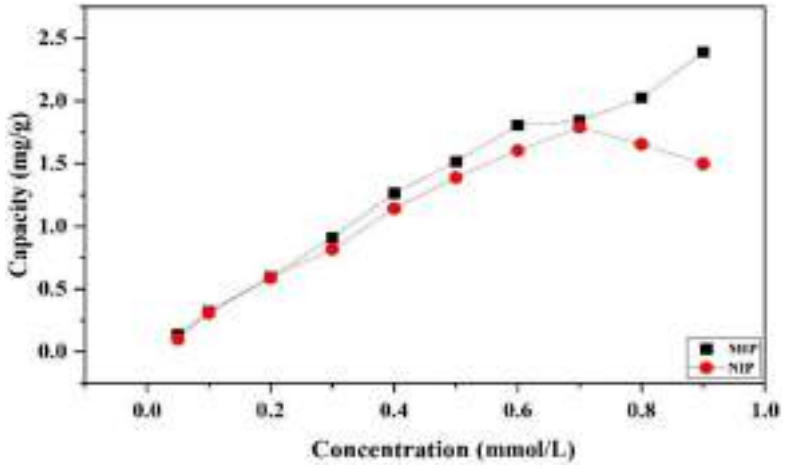

Fig. 6. Adsorption isotherm of LRZ on MIP and NIP.

Freundlich isotherm model, respectively. The linear Langmuir equation is illustrated in Eq. (5).

$$\frac{C_e}{Q_e} = \frac{1}{Q_{max}\, K_L} + \frac{C_e}{Q_{max}} \quad (5)$$

Where Q_{max} (mg/g) is the maximum adsorption isotherm for the polymer, and K_L is the constant for the Langmuir adsorption isotherm model. [30]

The results indicate that the adsorption of MIP towards LRZ follows the Freundlich isotherm model, which gives a linear equation equal to Log Q_e = 0.8397 Log C_e – 1.4789 with R^2 equal to 0.9768, while the NIP gives the linear equation Log Q_e = 0.3816 Log C_e – 0.7647 with R^2 equal to 0.2532, which is a higher R^2 than that obtained by applying the Langmuir model, as reported in Table 1, and illustrated in Fig. 7. This indicates that the Freundlich model provides a more accurate description of the binding mechanism, with the adsorption of LRZ adhering to a multimolecular layer physical adsorption process. [23,31] The Freundlich model is ideal for materials with heterogeneous binding site energies. [32] Additionally, the adsorption intensity values (1/n) for MIP and NIP were 0.8397 and 0.3816, respectively, indicating more favorable adsorption on MIP, where the value of 1/n serves as an indicator of the degree of favorability of adsorption, with n values greater than 1 signifying favorable conditions for adsorption. [33]

A kinetic adsorption experiment was conducted to study the rebinding efficiency of the synthesized polymer at a concentration of 0.4 mmol/L at different times, as illustrated in Fig. 8. It was observed that the amount of LRZ that interacts with the MIP increases over time up to 15 min, due to the presence of specific sites in the polymer for the selective LRZ binding. After 15 min, the amount of LRZ adsorbed by the polymers remains constant; this is expected when the system reaches adsorption equilibrium. [34,35]

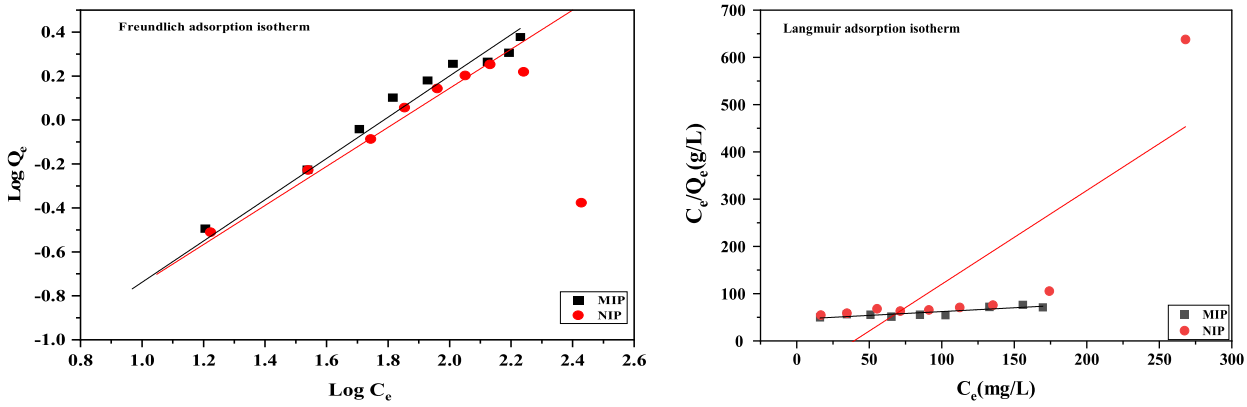

Fig. 7. Freundlich and Langmuir adsorption isotherm models for the adsorption of LRZ onto the prepared MIP and NIP.

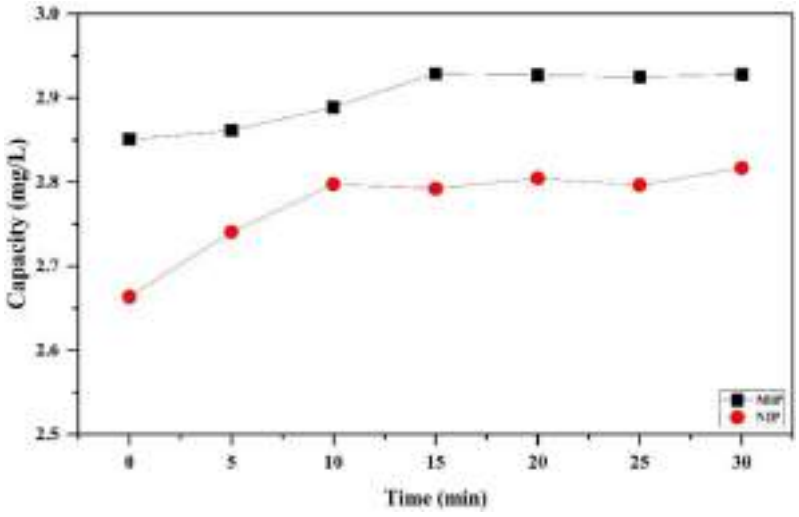

Fig. 8. Kinetics adsorption of MIP and NIP.

Table 1. Characteristics of the Freundlich and Langmuir adsorption isotherm models.

	Freundlich isotherm model		
Materials	K_F	n	R^2
MIP	0.033	1.19	0.9768
NIP	0.172	2.62	0.2532
	Langmuir isotherm model		
Materials	K_L	Q_{max} (mg/g)	R^2
MIP	283.44	6.16	0.7668
NIP	0.01	0.50	0.6664

The kinetics of adsorption was evaluated using the pseudo-first and second order according to the following Eqs. (6) and (7)):

$$\text{Pseudo} - \text{first} - \text{order equation}$$

$$\ln(Q_e - Q_t) = \ln Q_e - K_1 t \quad (6)$$

$$\text{Pseudo} - \text{second} - \text{order equation}$$

$$\frac{t}{Q_t} = \frac{1}{K_2\, Q_e^2} + \frac{t}{Q_t} \quad (7)$$

Where Qe refers to the adsorption quantity (mg/g) of LRZ at equilibrium time (min), Q_t refers to the amount of adsorption at time t (min), k_1 refers to the pseudo-first-order rate constant (1/min), and

Table 2. Kinetic parameters for the adsorption of LRZ on MIP and NIP.

			Pseudo – first – order			Pseudo – second – order		
Adsorbent	T (K)	q_e (mg/g)	q_e, cal (mg/g)	K_1 (1/min)	R^2	q_e, cal (mg/g)	K_2 (g/ mg.min)	R^2
MIP	298	2.929	0.115	0.154	0.9711	2.934	4.651	0.9999
NIP	298	2.816	0.099	0.089	0.7223	2.814	4.677	0.9999

$q_{e,exp}$ (mg/g) was measured by experiment; $q_{e,cal}$ (mg/g) was calculated by fitting.

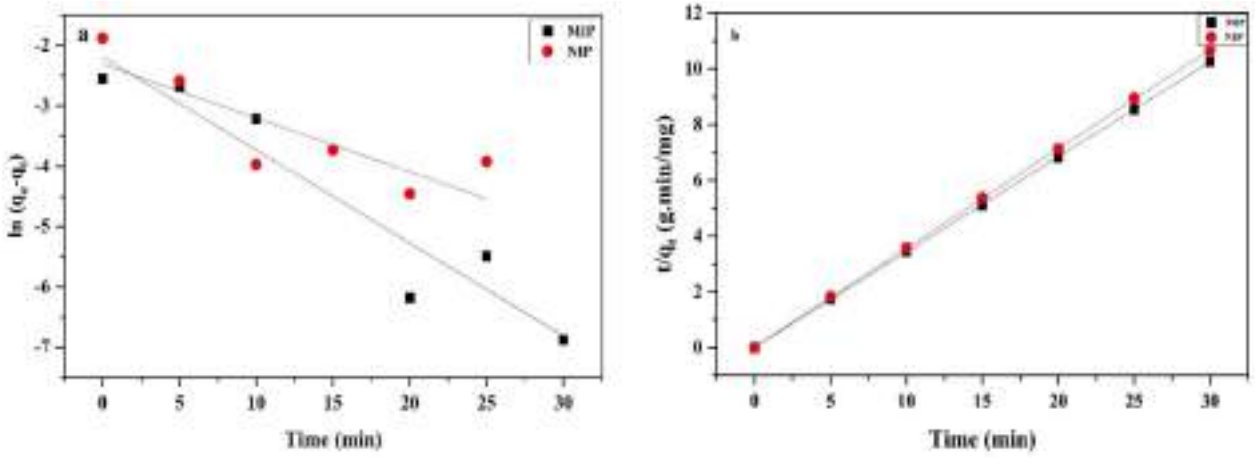

Fig. 9. Pseudo First and Second-Order Kinetic Models for MIP and NIP.

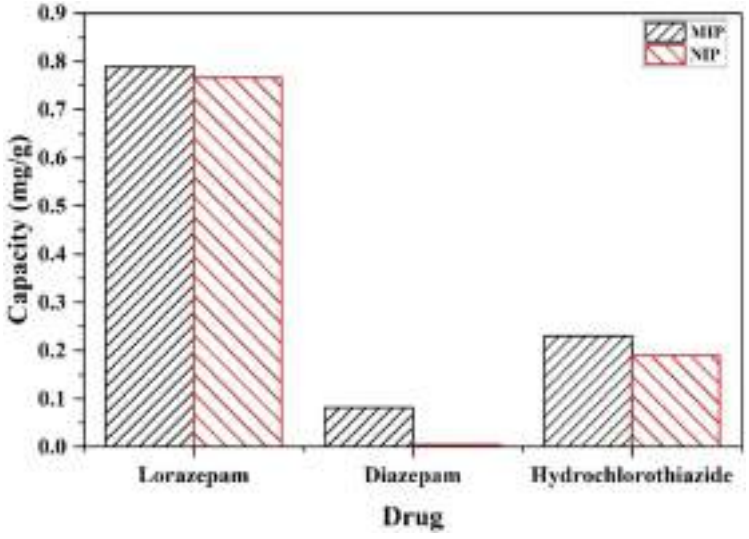

Fig. 10. Selectivity of MIP and NIP towards various analytes.

k_2 refers to the pseudo-second-order rate constant (g/ mg. min), respectively. The Fitted curves and related Kinetic parameters are present in Fig. 9 and Table 2, respectively. Based on the results, the pseudo–second–order kinetic model (R^2 = 0.9999) fit better than that of the pseudo-first-order (R^2 = 0.9117). It implies that chemical adsorption is the rate-controlling step for LRZ uptake on MIP. [36,37] This result is consistent with the Freundlich adsorption isotherm, which indicates that the adsorption process involves multiple interactions. The experimental values are also compatible with the predicted adsorption capacities obtained through the pseudo-second-order isotherm, in contrast to those predicted through the pseudo-first-order isotherm. [38]

Selectivity of polymers

Selectivity of MIPs is one of the main and outstanding advantages of MIPs. The selectivity of the

Table 3. Selectivity and imprinting factors for MIP and NIP towards various analytes.

Compound	Structure	Selectivity factor (α)	Imprinting Factor (IF)
Lorazepam	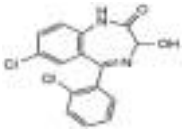	/	1.03
Diazepam	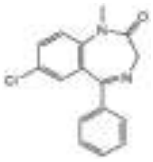	9.70	15.67
Hydrochlorothiazide	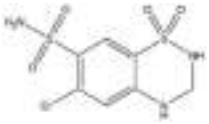	3.43	1.20

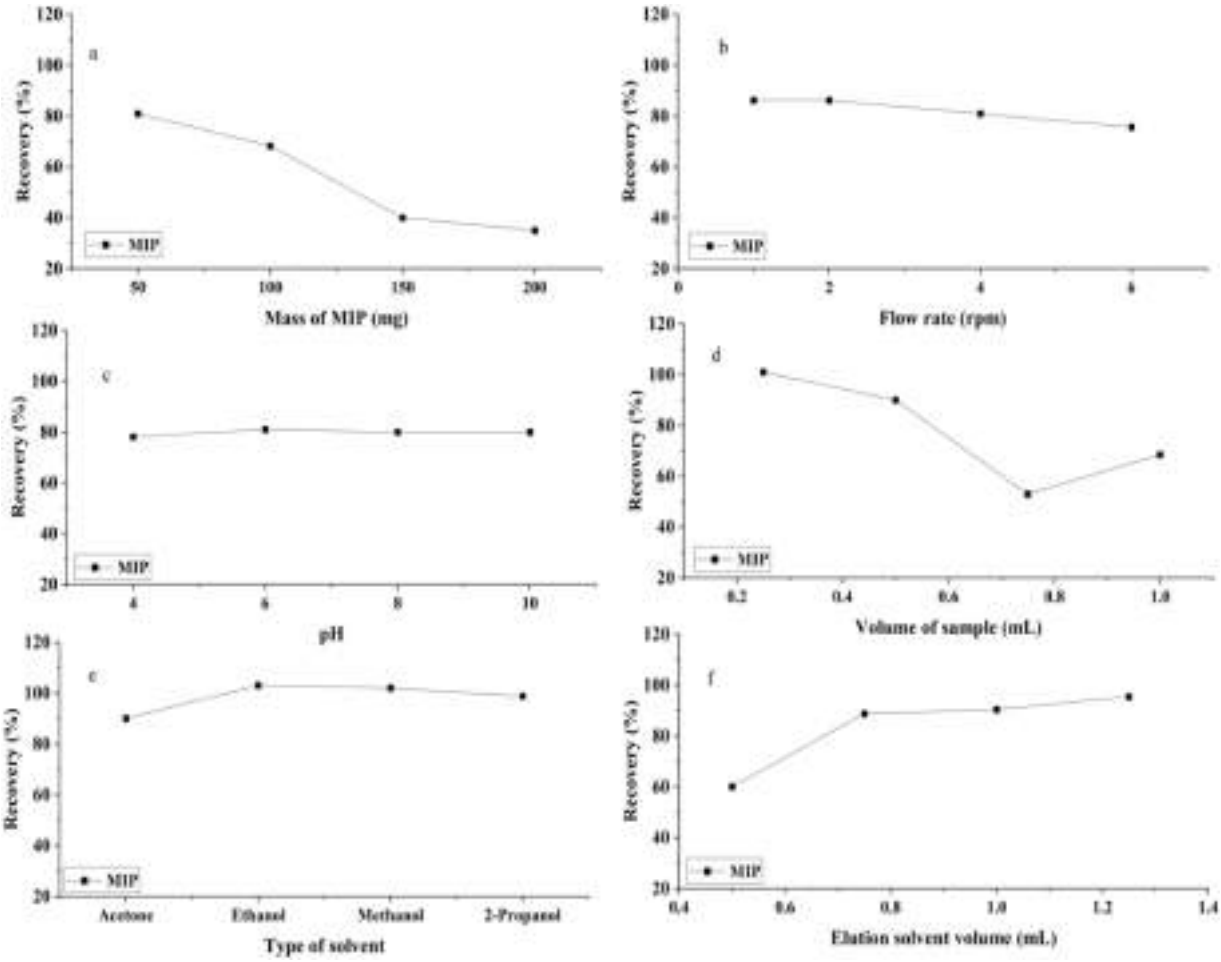

Fig. 11. Optimization of MIP-SPE parameters.

imprinted polymers is determined by the size, shape, and functional groups of the template molecule that integrates into the polymer structure during synthesis.[39] The selectivity of the synthesized MIP and NIP was evaluated using diazepam and hydrochlorothiazide as competitive drugs, as illustrated in Fig. 10.

The selectivity factor is obtained by comparing the adsorption capacities of MIP towards LRZ and an

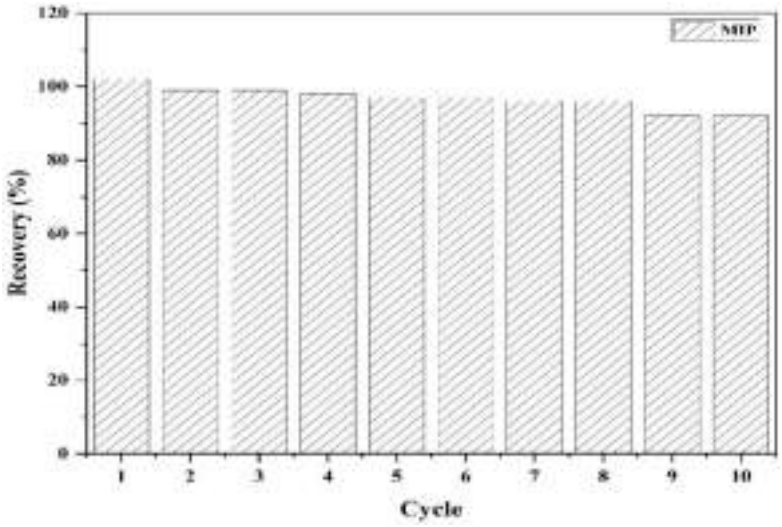

Fig. 12. Reusability of MIP.

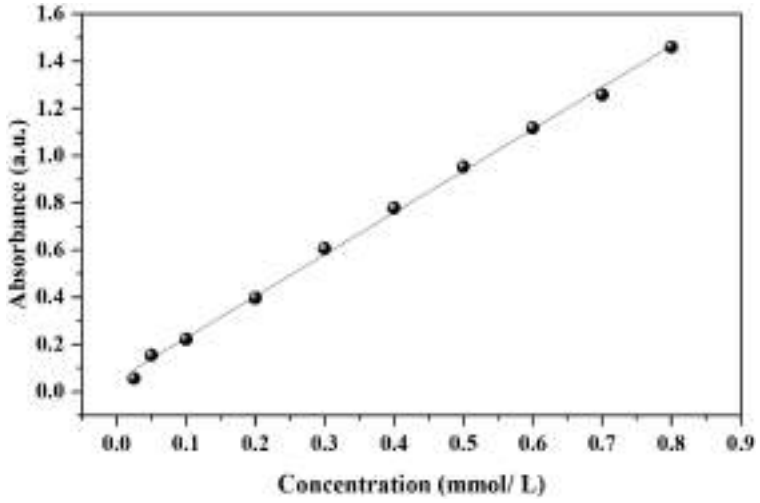

Fig. 13. Lorazépam calibration curve.

analogous analyte. The results indicate that the selectivity factor of MIP towards LRZ is found to be 15.67 and 1.20 against diazepam and hydrochlorothiazide, respectively. In contrast, the imprinting factor of the synthesized polymers (MIP/NIP) towards LRZ was found to be 1.03 by comparing the adsorption capabilities of the MIP and NIP at a concentration of 0.2 mmol/L for the analyte, as reported in Table 3. These results demonstrate that the developed method is selective for the determination of LRZ in various samples. Furthermore, the prepared MIP shows an acceptable imprinting factor. [40]

Table 4. Analytica data for the calibration curve.

Parameter	Value
Linear range (mmol/L)	0.025 – 0.8
Regression equation	A = 1.7679 C (mmol/L) + 0.0497
Maximum wavelength (nm)	319
Correlation of determination	0.9981
Correlation coefficient	0.9990
Repeatability RSD % n = 3	0.69
Reproducibility RSD % n = 3	0.72
Molar absorptivity (L/mol.cm)	1.7679×10^3
Sandell's sensitivity (μg/ cm^2)	5.56×10^{-4}
Limit of detection (μmol/L)	0.63
Limit of quantitation (μmol/L)	2.09

Optimization of solid phase extraction conditions

This study utilized MIP-SPE coupled with UV-Vis spectroscopy to extract and quantify LRZ in pharmaceutical and biological samples. To ensure optimal recovery of the analyte, the experimental parameters—including the amount of adsorbent, flow rate, sample volume, pH, and the type of elution solvent and its

Table 5. Results obtained for LRZ determination in pharmaceutical and biological samples.

Sample	Real / Spike (mmol/L)	Found* (mmol/L)	Recovery (%)	Absolute Error	Relative Error (%)	RSD %	Paired t-test
Tablet (2 mg)	0.2	0.202	101.00	0.002	1.00	0.86	2.04
	0.4	0.393	98.25	0.007	1.75	1.02	3.03
	0.6	0.587	97.83	0.013	2.16	1.05	3.63
Serum .1	0	-	-	-	-	-	-
	0.4	0.380	95.04	0.020	5.00	2.20	4.123
	0.6	0.577	96.16	0.038	3.83	2.38	2.907
Serum .2	0	-	-	-	-	-	-
	0.4	0.390	97.50	0.010	2.50	1.12	4.027
	0.6	0.581	96.83	0.019	3.16	1.66	3.464

* Average of three determinations, t-tab at confidence level 95%, n = 3, (4.303).

volume were thoroughly examined and optimized. The optimization was carried out using a solution containing 0.4 mmol/L of LRZ. The absorbance at a wavelength of 319 nm was utilized to assess the impact of the parameters on the recovery of the analyte.

Adsorbent mass

The packaging material's mass is a critical parameter in SPE due to the adsorption of the analyte onto it. In the adsorption process, adsorbent material quantities of 50, 100, 150, and 200 mg were assessed, as illustrated in Fig. 11a. The highest analytical signal was found when the sorbent mass was 50 mg; when the adsorbent mass increased after 50 mg, the analytical signal decreased as a result of the difficulty in sample passage and elution after 50 mg.[41] However, in subsequent experiments, the optimal quantity of packaging sorbent was 50 mg of MIP.

Flow rate

The flow rate was evaluated in this study in relation to the desorption of an analyte from MIP. In order to optimize the flow rate of the sample, a variety of flow rates using a peristaltic pump were investigated, ranging from 1 to 6 rpm. The results indicated that the efficacy of LRZ desorption increased until the flow rate reached 2 rpm, and decreased as the flow rate increased to 6 rpm, as illustrated in Fig. 11b. This is attributed to the reduced contact between the adsorbent and the elution solvent at high flow rates.[42,43] So, the flow rate of 2 rpm was chosen for the subsequent experiments.

pH of the sample

The pH of the sample was a crucial factor in determining the adsorption and subsequent recovery of the analytes.[33] To investigate the impact of pH, LRZ solutions with a concentration of 0.4 mmol/L were changed to pH values ranging from 2 to 8 using 1 mol/L HCl and NaOH. The extraction of LRZ was evaluated for 0.5 mL of each solution, including an untreated LRZ solution at pH 6, using 50 mg of MIP, as depicted in Fig. 11c. Extraction efficiency was largely unaffected by pH, with optimum recovery observed at neutral pH. The optimal efficiency observed at neutral pH, this is attributed to the neutral form of LRZ and the H-bonding interaction between the template and cavities of MIP.[37,39,44] Consequently, a pH of 6.0 was selected for all subsequent studies.

Sample volume

The sample volume is a critical parameter in the optimization of MIP-SPE, as it directly affects the interaction between the target analyte and the imprinted binding sites. Sample volumes ranging from 0.25 to 1.0 mL were assessed in this investigation. The highest recovery was achieved with a sample volume of 0.25 mL, as illustrated in Fig. 11d. This can be attributed to the favorable ratio between the quantity of analyte and the available sorbent binding sites. In recent studies, comparable findings have been reported wherein excessive sample loading resulted in reduced recoveries as a result of sorbent saturation and restricted accessibility of imprinting sites.[44]

Elution solvent type and volume

For MIP in SPE, the template molecules need to be removed to be quantified by using UV-Visible spectroscopy, so the eluent species are crucial. The main mechanism is that the eluent solvent destroys the interaction between the template molecule and the functional monomer, weakening the binding between them and eluting the template molecules. A study was conducted to select the best solvent for efficiently desorbing LRZ from MIP while maintaining

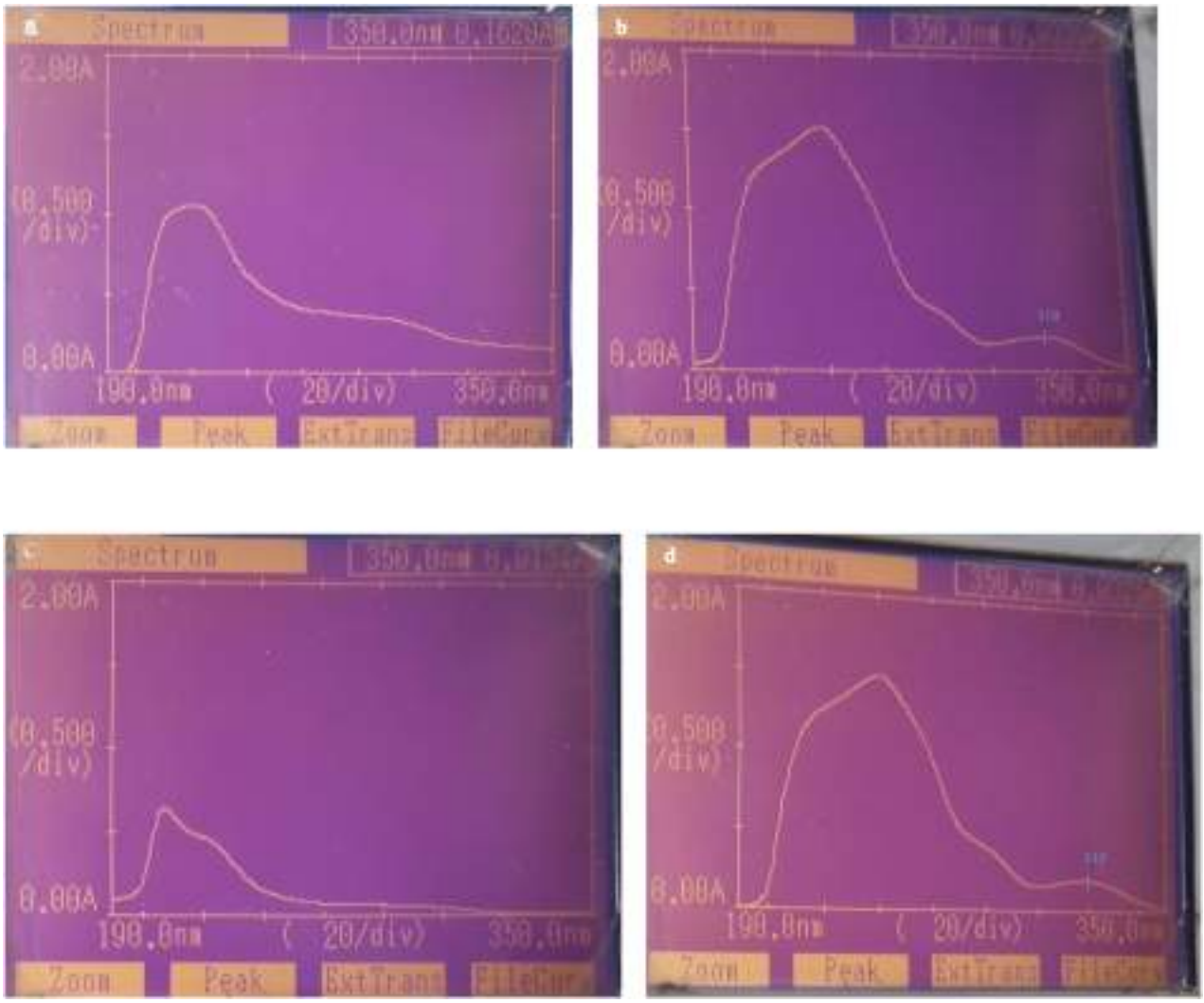

Fig. 14. Application of MIP-SPE to serum samples. (a, b) Unspiked and spiked (0.6 mmol/L LRZ) serum sample 1; (c, d) Unspiked and spiked (0.6 mmol/L LRZ) serum sample 2, respectively.

high recovery rates. The elution of LRZ from MIP was tested using four solvents: acetone, ethanol, methanol, and 2-propanol. The concentration of LRZ in each solvent was measured using UV-visible spectroscopy, as shown in Fig. 11e. Ethanol was chosen as the best solvent for extracting LRZ from MIP due to its better efficacy. As a result, it was chosen as the elution solvent for future studies. The volume of elution solvent was changed from (0.5, 0.75, 1, and 1.25 mL). Fig. 11f shows that a volume of 1.25 mL was best for eluting LRZ.

Reusability of MIP

Reusability is a key parameter of LRZ-MIP for practical applications. To assess the reusability of the synthesized MIP, the MIP with LRZ was extracted with a solution of ethanol: acetic acid (90:10, v/v) to elute the LRZ. The regenerated MIP was subsequently employed to re-adsorb LRZ. The elution/adsorption cycle was continuously carried out ten times under the optimum conditions (n = 10). Following ten regeneration cycles, the effectiveness of analyte recovery decreases by 8%, as shown in Fig. 12, possibly due to the degradation or obstruction of the binding sites. These results demonstrate that the MIP exhibits satisfactory reusability.[24]

Analytical parameters

The linearity, precision, limit of detection (LOD), and limit of quantitation (LOQ) of the proposed method were evaluated using LRZ standard solutions.

The results are presented in Table 4. A linear least-squares regression of the absorbance of LRZ versus concentration in triplicate was used to develop the calibration curve over the range of 0.025 to 0.8 mmol/L. The calibration curve exhibited a correlation coefficient of r = 0.9990, indicating excellent linearity, as shown in Fig. 13. The relative standard deviation (RSD%) was calculated for intra-day and inter-day (n = 3) measurements to assess the method's precision. The values were 0.69% and 0.72%, respectively.

The LOD is the lowest concentration of an analyte that can be detected above the background noise. The limit of quantification (LOQ) is the smallest amount of an analyte in a sample that can be measured with acceptable precision and accuracy. The calculated LOD and LOQ were found to be 0.63 and 2.09 μmol/L, respectively. The results suggest that the proposed spectrophotometric method offers an easy, rapid, and highly sensitive way to determine LRZ.

Application to real samples

The proposed method using MIP as an adsorbent material in solid phase extraction was applied for the extraction and determination of LRZ in pharmaceutical and biological samples, as reported in Table 5. The reliability of the suggested method was considered by direct determination of LRZ in a pharmaceutical sample at three concentration levels (0.2, 0.4, and 0.6) mmol/L. Furthermore, the extraction of the drug from a serum sample from a healthy volunteer was established by spiking the sample with two concentration levels of LRZ (0.4, and 0.6) mmol/L, as illustrated in Fig. 14. The percentage recoveries were found to be quantitative in the range of 95.0–101.0%, with a relative standard deviation (RSD%) of <2.5%. The results indicate the effectiveness of the method for the extraction and determination of LRZ in pharmaceutical and biological samples.

Comparison with previous studies

The analytical characteristics of the MIP-SPE-UV-Visible spectroscopy method were compared to methods previously reported in the literature for the extraction and determination of LRZ in various sample matrices, as reported in Table 6. The developed method provided a linear calibration curve in the millimolar concentration range, which is higher than that of other methods. Although MIP–SPE significantly improves selectivity and reduces matrix interference, the detection capability remains lower compared to chromatographic or electrochemical methods, which typically achieve nanomolar or ppm detection limits due to signal amplification and higher instrumental sensitivity. Thus, the present method is more suitable for routine analysis where moderate sensitivity with high selectivity and cost-effectiveness are required. [45,46]

Table 6. Comparison for the determination of LRZ with other methods.

Technique	Method	Linear range	LOD	LOQ	Recovery (%)	RSD (%)	Sample	Ref.
Amperometry	Electrochemical detection using GCE coated with electropolymerized-MIP, modified with MWCNTs and AuNPs	0.5–1.0 and 1.0–10 nM	0.2 nM	/	>96	3.8	Biological samples	[47]
Potentiometry	Electrochemical sensor using PGE modified with a nanocomposite of polypyrrole@sol–gel@AuNPs and MIP	0.2–2.0 nM 2.0–20.0 nM	0.09 nM	/	>96	3.2	Pharmaceuticals and biological samples	[48]
High-performance liquid chromatography	chromatographic determination after extraction of lorazepam (and clonazepam) using nano-sponge activated carbon.	0.006–10 ppm	0.0013 ppm	0.004 ppm	>84	<5.5	Environmental and biological samples	[49]
UV-Visible spectroscopy	Spectroscopic determination based on MIP-SPE	0.025–0.8 mmol/L	0.63 μmol/L	2.09 μmol/L	>95	<2.5	Pharmaceuticals and biological samples	This work

Conclusion

This study presents a new approach for the separation and quantification of LRZ by integrating molecular imprinting polymer-solid phase extraction with UV-visible spectroscopy. Characterization of the polymers revealed significant properties for the synthesis of MIP, with the surfaces exhibiting heterogeneous and irregular morphologies, good thermal stability, and higher selectivity for the target analyte. Furthermore, the synthesized MIP exhibits good reusability under optimal conditions. Molecular imprinting polymer-solid phase extraction coupled with UV-Visible spectroscopy demonstrated sufficient sensitivity and reproducibility. Furthermore, the method has a rapid and effortless implementation, with minimal solvent usage. The method was successfully applied to the extraction and determination of LRZ in pharmaceutical and biological samples with acceptable recoveries.

Authors' declaration

- Conflicts of Interest: None.
- We hereby confirm that all Figures and Tables in the manuscript are ours. Furthermore, any Figures and images that are not ours have been included with the necessary permission for republication, which is attached to the manuscript.
- No animal studies are present in the manuscript.
- No human studies are present in the manuscript.
- Ethical Clearance: The project was approved by the local ethical committee at the University of Baghdad.

Authors' contributions statement

All authors contributed to the study conception and design. Material preparation, data collection, and analysis were performed by E. W. A., Y. K. A. The first draft of the manuscript was written by E. W. A. and revised by Y. K. A.

References

1. Chinna P, Prakash MS, Ramakrishna RA, Sreenivasa S, Singh Y. Quantification of Genotoxic Impurities by HPLC in Active Pharmaceutical Ingredient Lorazepam. J Anal Chem. 2023; 78(4):514-521. https://doi.org/10.1134/S106193482304007X
2. Banaszkiewicz L, Woźniak MK, Kata M, Domagalska E, Wiergowski M, Szpiech B, *et al.* Rapid and simple multi-analyte LC–MS/MS method for the determination of benzodiazepines and Z-hypnotic drugs in blood samples: Development, validation and application based on three years of toxicological analyses. J Pharm Biomed Anal. 2020;191:113569. https://doi.org/10.1016/j.jpba.2020.113569
3. Bolte K, Dziadosz M, Kono N, Vennemann B, Klintschar M, Teske J. Determination of drugs in exhumed liver and brain tissue after over 9 years of burial by liquid chromatography-tandem mass spectrometry—Part 1: Cardiovascular drugs. Drug Test Anal. 2021;13(3):595-603. https://doi.org/10.1002/dta.2940
4. Caballero-Casero N, Mihretu LD, Rubio S. Interference-Free Method for Determination of Benzodiazepines in Urine Based on Restricted-Access Supramolecular Solvents and LC–MS-MS. J Anal Toxicol. 2022;46(3):285-294. https://doi.org/10.1093/jat/bkab023
5. Cobo-Golpe M, de-Castro-Ríos A, Cruz A, Páramo M, López-Rivadulla M, Lendoiro E. Determination of antidepressants and benzodiazepines in paired hair and nail samples. Forensic Sci Int. 2021;326:110935. https://doi.org/10.1016/j.forsciint.2021.110935
6. Choudhary P, Bansal S, Verma KL. HPTLC–MS method for the determination of benzodiazepines in urine samples. J Planar Chromatogr - Mod TLC. 2020;33(5):523-530. https://doi.org/10.1007/s00764-020-00053-w
7. Jain B, Jain R, Kabir A, Ghosh A, Zughaibi T, Chauhan V, *et al.* Cellulose Paper Sorptive Extraction (CPSE) Combined with Gas Chromatography–Mass Spectrometry (GC–MS) for Facile Determination of Lorazepam Residues in Food Samples Involved in Drug Facilitated Crimes. Separations. 2023;10(5). https://doi.org/10.3390/separations10050281
8. Banaszkiewicz L, Woźniak MK, Kaliszan M, Kot-Wasik A. Determination of benzodiazepines and Z-hypnotic drugs in whole blood samples by GC–MS/MS: Method development, validation and application. Microchem J. 2023;193:109115. https://doi.org/10.1016/j.microc.2023.109115
9. Ghorbanpoor S, Shishehbor MR, Sheibani A, Safaei M, Nazari A. Determination of Lorazepam in Drug Formulation and Biofluids Using a Spectrophotometric Method and Response Surface Methodology. J Appl Spectrosc. 2020;87(5):965-975. https://doi.org/10.1007/s10812-020-01096-x
10. Zankanah FH, Al Ani FA, Shaker AR, Abdulraheem MS. First- and Second-Derivative Spectrophotometry for Simultaneous Determination of lorazepam and clonazepam in pharmaceutical formulations. Egypt. J Chem. 2023;66(3):271-280. https://doi.org/10.21608/ejchem.2022.130646.5753
11. Hashemi SH, Kaykhaii M. Porous Polymer Sorbents in Micro Solid Phase Extraction: Applications, Advantages, and Challenges. Top Curr Chem. 2024;382(4):37. https://doi.org/10.1007/s41061-024-00481-w
12. Zhao G, Zhang Y, Sun D, Yan S, Wen Y, Wang Y, *et al.* Recent Advances in Molecularly Imprinted Polymers for Antibiotic Analysis. Molecules. 2023;28(1). https://doi.org/10.3390/molecules28010335
13. Aldeen RAK, Al-Bayati YK. Selective Extraction of Metformin in Pharmaceutical Preparation via Synthesized MIP-SPE Techniqu. Iraqi J Sci. 2023;64(8):3763-3778. https://doi.org/10.24996/ijs.2023.64.8.4
14. Hassoon GS, Al-Bayati YK. Synthesis, Characterization and Application of Calcium Ion-Imprinted Polymeric Solid-Phase Extraction and Pre-Concentration in Aqueous Solutions by Packed-Bed Columns. Iraqi J Sci. 2023;64(11):5462-5475. https://doi.org/10.24996/ijs.2023.64.11.1
15. Al-Bayati YK, Al-Safi AJ. Synthesis and Characterization of a Molecularly Imprinted Polymer for Diclofenac Sodium Using (2-vinylpyridine and 2-hydroxyethyl metha acrylate) as the Complexing Monomer. Baghdad Sci J. 2018;15(1):1. http://dx.doi.org/10.21123/bsj.2018.15.1.0063

16. Haji Abdolrasouli M, Ali R, Hamid A, and Mohammadiazar S. Determination of Lorazepam and Diazepam Using Modified Nanocrystalline Cellulose for Ultrasonic-Assisted Dispersive Solid Phase Microextraction (UA-DSPME) and Gas Chromatography-Mass Spectrometry (GC-MS). Anal Lett. 2024;57(13):2085-2102. https://doi.org/10.1080/00032719.2023.2285864
17. Jiang Y, Qiu X, Zhao X, Fu Y, Su W, Li Y, *et al.* Preparation and optimization of dummy molecularly imprinted polymer-based solid-phase extraction system for selective enrichment of p-toluene sulfonate esters genotoxic impurities. J Chromatogr. 2024;1728:465029. https://doi.org/10.1016/j.chroma.2024.465029
18. Liang A, Lv T, Pan B, Zhu Z, Haotian R, Xie Y, *et al.* Dynamic simulation and experimental studies of molecularly imprinted label-free sensor for determination of milk quality marker. Food Chem. 2024;449:139238. https://doi.org/10.1016/j.foodchem.2024.139238
19. Al Faysal A, Cetinkaya A, Erdoğan T, Ozkan SA, Gölcü A. Comparative study of two MIP-based electrochemical sensors for selective detection and quantification of the antiretroviral drug lopinavir in human serum. Talanta. 2025;281:126791. https://doi.org/10.1016/j.talanta.2024.126791
20. Milani Hosseini MR, Motaharian A. Electroanalytical determination of diazepam in tablet and human serum samples using a multiwalled carbon nanotube embedded molecularly imprinted polymer-modified carbon paste electrode. RSC Advances. 2015;5(99):81650-81659. https://doi.org/10.1039/C5RA11598A
21. Bichan MJ, Al-Bayati YK, Al-Abady FM, Awwadi FF. Theoretical study of molecularly imprinted polymers prepared for homatropine methylbromide. J Polym Res. 2023;30(4):142. https://doi.org/10.1007/s10965-023-03513-z
22. Abood ME, Abbas SM. Molecular imprinted of nylon 6 for selective separation of procaine by solid-phase extraction. Indones J Chem. 2021;21(6):1505-1513. https://doi.org/10.22146/ijc.66997
23. Karrat A, Palacios-Santander JM, Amine A, Cubillana-Aguilera L. A novel magnetic molecularly imprinted polymer for selective extraction and determination of quercetin in plant samples. Anal Chim Acta. 2022;1203:339709. https://doi.org/10.1016/j.aca.2022.339709
24. Cao Y, Huang Z, Luo L, Li J, Li P, Liu X. Rapid and selective extraction of norfloxacin from milk using magnetic molecular imprinting polymers nanoparticles. Food Chem. 2021;353:129464. https://doi.org/10.1016/j.foodchem.2021.129464
25. Suryana S, Mutakin M, Rosandi Y, Hasanah AN. Molecular Dynamic Study of Mechanism Underlying Nature of Molecular Recognition and the Role of Crosslinker in the Synthesis of Salmeterol-Targeting Molecularly Imprinted Polymer for Analysis of Salmeterol Xinafoate in Biological Fluid. Molecules. 2022;27(11). https://doi.org/10.3390/molecules27113619
26. Cui Y, Su A, Feng J, Dong W, Li J, Wang H, *et al.* Development of silica molecularly imprinted polymer on carbon dots as a fluorescence probe for selective and sensitive determination of cetirizine in saliva and urine. Spectrochim Acta A Mol Biomol Spectrosc. 2022;264:120293. https://doi.org/10.1016/j.saa.2021.120293
27. Wisnuwardhani HA, Ibrahim S, Mukti RR, Damayanti S. Study on monomer functional suitability toward sofosbuvir in molecularly imprinted polymer: In silico and experimental study. Composites Part C: Open Access. 2023;12:100405. https://doi.org/10.1016/j.jcomc.2023.100405
28. Nurlin Abu Samah SMAA, Gaanty Pragas M. Synthesis and Characterization of Molecular Imprinted Polymer in Oleic acid Isolation from Palm Fatty Acid Distillate Wastes Malaysian Journal of Analytical Sciences. 2023;27(1):20–29.
29. Foroughirad S, Haddadi-Asl V, Khosravi A, Salami-Kalajahi M. Effect of porogenic solvent in synthesis of mesoporous and microporous molecularly imprinted polymer based on magnetic halloysite nanotubes. Materials Today Communications. 2021;26:101780. https://doi.org/10.1016/j.mtcomm.2020.101780
30. Nguyen V-T, Giang HH, Tran TTN, Van T-K, Tran T. Synthesis and Characteristics of Polymer-Mediated Curcumin Molecular Imprinting for Quantitative Determination of Curcumin in Food Samples. J Chromatogr. 2024;1713:464567. https://doi.org/10.1016/j.chroma.2023.464567
31. Sadegh N, Asfaram A, Javadian H, Haddadi H, Sharifpour E. Ultrasound-assisted solid phase microextraction-HPLC method based on Fe3O4@SiO2-NH2-molecularly imprinted polymer magnetic nano-sorbent for rapid and efficient extraction of harmaline from Peganum harmala extract. J Chromatogr B. 2021;1171:122640. https://doi.org/10.1016/j.jchromb.2021.122640
32. Abu-Alsoud GF, Hawboldt KA, Bottaro CS. Comparison of Four Adsorption Isotherm Models for Characterizing Molecular Recognition of Individual Phenolic Compounds in Porous Tailor-Made Molecularly Imprinted Polymer Films. ACS Applied Materials & Interfaces. 2020;12(10):11998-12009. https://doi.org/10.1021/acsami.9b21493
33. Karrat A, Amine A. Solid-phase extraction combined with a spectrophotometric method for determination of Bisphenol-A in water samples using magnetic molecularly imprinted polymer. Microchem J. 2021;168:106496. https://doi.org/10.1016/j.microc.2021.106496
34. Martins RO, Gomes IC, Mendonça Telles AD, Kato L, Souza PS, Chaves AR. Molecularly imprinted polymer as solid phase extraction phase for condensed tannin determination from Brazilian natural sources. J Chromatogr. 2020;1620:460977. https://doi.org/10.1016/j.chroma.2020.460977
35. He Q, Liang J-J, Chen L-X, Chen S-L, Zheng H-L, Liu H-X, *et al.* Removal of the environmental pollutant carbamazepine using molecular imprinted adsorbents: Molecular simulation, adsorption properties, and mechanisms. Water Res. 2020;168:115164. https://doi.org/10.1016/j.watres.2019.115164
36. Hatamluyi B, Sadeghian R, Malek F, Boroushaki MT. Improved solid phase extraction for selective and efficient quantification of sunset yellow in different food samples using a novel molecularly imprinted polymer reinforced by Fe3O4@UiO-66-NH2. Food Chem. 2021;357:129782. https://doi.org/10.1016/j.foodchem.2021.129782
37. Xolo T, Mahlambi P. Molecularly imprinted polymers as solid-phase and dispersive solid-phase extraction sorbents in the extraction of antiretroviral drugs in water: adsorption, selectivity and reusability studies. Journal of Analytical Science and Technology. 2024;15(1):11. https://doi.org/10.1186/s40543-024-00418-4
38. Khulu S, Ncube S, Kgame T, Mavhunga E, Chimuka L. Synthesis, characterization and application of a molecularly imprinted polymer as an adsorbent for solid-phase extraction of selected pharmaceuticals from water samples. Polym Bull. 2022;79(2):1287-1307. https://doi.org/10.1007/s00289-021-03553-9
39. Jalilian N, Ebrahimzadeh H, Asgharinezhad AA, Khodayari P. Magnetic molecularly imprinted polymer for the selective dispersive micro solid phase extraction of phenolphthalein in urine samples and herbal slimming capsules prior to HPLC-PDA analysis. Microchem J. 2021;160:105712. https://doi.org/10.1016/j.microc.2020.105712

40. Agibayeva L, Melnikov Y, Berdaly A, Kondaurov R. Development of Optimal Conditions for Synthesis of Molecularly Imprinted Polymers for Effective Terbium Sorption. Polymers. 2025;17(10). https://doi.org/10.3390/polym17101398
41. Tamandani M, Hashemi SH, Kaykhaii M, Jamali Keikha A, Nasiriyan A. Determination of profenofos in seawater and foodstuff samples after its molecularly imprinted polymer pipette-tip micro solid phase extraction optimized by response surface methodology. BMC Chemistry. 2022;16(1):12. https://doi.org/10.1186/s13065-022-00807-z
42. Davarani SSH, Rezayati zad Z, Taheri AR, Rahmatian N. Highly selective solid phase extraction and preconcentration of Azathioprine with nano-sized imprinted polymer based on multivariate optimization and its trace determination in biological and pharmaceutical samples. Mater Sci Eng C. 2017; 71:572-583. https://doi.org/10.1016/j.msec.2016.09.075
43. Dourado CS, Domingues IFF, de Oliveira Magalhães L, Casarin F, Ribeiro ML, Braga JWB, *et al.* Optimization of a saccharin molecularly imprinted solid-phase extraction procedure and evaluation by MIR hyperspectral imaging for analysis of diet tea by HPLC. Food Chem. 2022;367:130732. https://doi.org/10.1016/j.foodchem.2021.130732
44. Dinali LAF, de Oliveira HL, Teixeira LS, da Silva ATM, D'Oliveira KA, Cuin A, *et al.* Efficient development of a magnetic molecularly imprinted polymer for selective determination of trimethoprim and sulfamethoxazole in milk. Microchem J. 2020;154:104648. https://doi.org/10.1016/j.microc.2020.104648
45. Silva RCdS, Pires BC, Borges KB. Double-imprinted polymer based on cross-linked poly(vinylimidazole–trimethylolpropane trimethacrylate) in solid phase extraction for determination of lead from wastewater samples by UV–vis spectrophotometry. Int J Environ Anal Chem. 2019;99(10): 949-967. https://doi.org/10.1080/03067319.2019.1616717
46. Mabrouk M, Hammad SF, Abdella AA, Mansour FR. Chitosan-based molecular imprinted polymer for extraction and spectrophotometric determination of ketorolac in human plasma. Spectrochim Acta A Mol Biomol Spectrosc. 2020;241:118668. https://doi.org/10.1016/j.saa.2020.118668
47. Rezaei B, Rahmanian O, Ensafi AA. Sensing Lorazepam with a glassy carbon electrode coated with an electropolymerized-imprinted polymer modified with multiwalled carbon nanotubes and gold nanoparticles. Microchimica Acta. 2013;180(1):33-39. https://doi.org/10.1007/s00604-012-0897-z
48. Rezaei B, Boroujeni MK, Ensafi AA. A novel electrochemical nanocomposite imprinted sensor for the determination of lorazepam based on modified polypyrrole@sol-gel@gold nanoparticles/pencil graphite electrode. Electrochim Acta. 2014;123:332-339. https://doi.org/10.1016/j.electacta.2014.01.056
49. Khodadoust S, Talebianpoor MS. Optimization of the extraction of clonazepam and lorazepam using nano-sponge activated carbon and its determination by high-performance liquid chromatography. Microchem J. 2024;207:111937. https://doi.org/10.1016/j.microc.2024.111937

الاستخلاص الانتقائي المعتمد على الطبعة البوليمرية الجزيئية لتقدير اللورازيبام في العينات الصيدلانية و البايولوجية

ايمان وجيه أمين[1،2]، يحيى كمال البياتي[1]

[1] قسم الكيمياء، كلية العلوم، جامعة بغداد، بغداد، العراق.
[2]هيئة البحث العلمي، بغداد، العراق.

الخلاصة

تم تقييم طريقة جديدة وانتقائية لفصل وتقدير اللورازيبام في نماذج صيدلانية باستخدام الطبعة البوليمرية الجزيئية كمادة امتزاز للاستخلاص بالطور الصلب. حضرت الطبعة البوليمرية بواسطة بلمرة الجذور الحرة باستخدام اللورايبام كقالب والاكريل أمايد كمونمر. شخصت البوليمرات المحضرة باستخدام جهاز الاشعة المرئية – فوق البنفسجية وطيف الاشعة تحت الحمراء والمجهر الالكتروني الماسح والتحليل الحراري الوزني. تم دراسة الامتزاز الايزوثيرمي والحركية لتشخيص امتزاز اللورازيبام بواسطة البوليمرات المحضرة بالإضافة الى تشخيص الانتقائية وإعادة الاستخدام لبوليمر الطبعة الجزيئية. تم دراسة العوامل المؤثرة على الاستخلاص بالطور الصلب منها وزن المادة البولمرية ومعدل الجريان والدالة الحامضية وحجم العينة ونوع وحجم المذيب المستخدم لإزاحة المادة الدوائية. أعطت الطريقة المقترحة مدى خطي يتراوح ما بين 0.025 – 0.8 ملي مول/لتر مع معامل ارتباط 0.9990. تم تقدير حد الكشف النوعي والكمي ليكون 0.63 و2.09 مايكرومول /لترعلى التوالي. تم تطبيق الطريقة المقترحة لفصل وتقدير اللورازيبام في النماذج الصيدلانية و البايولوجية باسترجاعية بحدود95-101 % مع معامل انحراف خطي اقل من 2.5 %.

الكلمات المفتاحية: الامتزاز الإيزوثيرمي، لورازيبام، الطبعة البوليمرية الجزيئية، الاستخلاص بالطور الصلب، مطياف الاشعة المرئية – فوق البنفسجية.